

## Pulse fitting and spectral analysis of short gamma-ray bursts and the magnetar giant flare, GRB200415A

---

**D. J. Maheso\* and S. Razzaque**

*Centre for Astro-Particle Physics (CAPP) and Department of Physics  
University of Johannesburg, P. O. BOX 524, Auckland Park 2006, South Africa*

*E-mail: [d.j.maheso@gmail.com](mailto:d.j.maheso@gmail.com)*

We present pulse fitting and spectral analysis of eight short gamma-ray bursts (SGRBs) and one magnetar giant flare (MGF), GRB200415A, that were all detected by the *Fermi* Gamma-ray Burst Monitor and have known redshift. GRB200415A is an MGF misclassified as an SGRB because its temporal structure resembles that of SGRBs. This difficulty in distinguishing between SGRBs and MGFs hinders cosmological studies. To address this, we used pulse rise times and the power law spectral index to differentiate the two transients. Their pulses were fitted with the Norris function revealing that GRB200415A has rapid pulse rise times, while the SGRBs have slower pulse rise times. Additionally, their spectra was fitted with a power law model that has an exponential cutoff, which breaks at a few MeV for both SGRBs and the MGF. We also found that the MGF has the hardest power law index, which explains its thermal-like emission.

*High Energy Astrophysics in Southern Africa 2022 - HEASA2022  
28 September - 1 October 2022  
Brandfort, South Africa*

---

\*Speaker

## 1. Introduction

Short gamma-ray bursts (SGRBs) and magnetar giant flares (MGFs) are short gamma-ray transients (SGRTs) that are short-lived, with 90% of their emission lasting less than 2 s (i.e.  $T_{90} < 2$  s). SGRBs are one of the most luminous events [1] and they are cosmological sources originating from compact binary mergers. MGFs, on the other hand, originate from magnetars within the Milky Way and nearby star-forming galaxies. Magnetars were first detected in the 1970s [2]. When they are observed from cosmological distances they can be misclassified as SGRBs. As a result they are given GRB designations, like the MGF detected on the 15<sup>th</sup> of April, 2020, which was designated as GRB200415A.

Typically, SGRBs show one prominent peak in their temporal structure, while MGFs consists of a prominent peak and an extended oscillating phase. However, when MGFs are observed from cosmological distances, their oscillating pulses are not observed, and their light curves show only the prominent peak. Burns et al. [3] found that MGFs misclassified as SGRBs have pulses that rise within a few tens of milliseconds. In this work we study the pulse rise time of SGRBs and the MGF, GRB200415A, to distinguish between the two.

MGFs are galactic sources and they can hinder cosmological studies if they are misclassified as cosmological SGRBs. Therefore, distinguishing these two types of SGRTs is crucial. This study aims to differentiate between MGFs and SGRBs by studying their temporal structures and spectral features. The transients pulses will be fit with the Norris function [4] to retrieve their rise times. Both types of transients are spectrally hard, and their spectra are usually best fit with a power law (PL) that has an exponential cutoff, and this spectral model is known as the Comptonised (Comp) model. The cutoff energy of these transients when fit with the Comp model occurs at a few MeV [5].

## 2. Methods

### 2.1 Instrumentation summary

We analysed sources detected by the *Fermi* Gamma-ray Burst Monitor (GBM) instrument of the *Fermi* Telescope. The instrument consists of two types of detectors: twelve sodium iodide (NaI) and two bismuth germanate oxide (BGO) scintillation detectors (see the instrumentation paper [6] for more details). NaI is sensitive to photons within the energy range  $\sim 10$  keV – 1 MeV, while BGO is sensitive to photons with the energy of  $\sim 200$  keV – 40 MeV. This instrument is ideally suited to detect these short, hard bursts due to its low photon energy sensitivity.

### 2.2 Data selection

Between 2008 and 2022, the *Fermi*-GBM was triggered by 362 SGRBs, but only nine had known redshift including the MGF, GRB200415A. Therefore, our sample consists of time-tagged data events with known redshift for the eight SGRBs and the MGF, GRB200415A, all of which were retrieved from the HEASARC browse interface<sup>1</sup>.

---

<sup>1</sup><https://heasarc.gsfc.nasa.gov/FTP/fermi/data/gbm/bursts/>

### 2.3 Triggered detectors and energy selection

The brightest NaI and BGO detectors for each transient was selected using *version 03 – 00 – 00p5* of the *gtburst* python graphical user interface from the *Fermi* Science Support Center *fermi-tools*<sup>2</sup>. This was accomplished by choosing detectors triggered by gamma-ray photons at incidence angles  $< 60^\circ$ . Ten energy channels were used in the temporal analysis of SGRTs: six from the NaI detectors and four from the BGO detectors. The NaI energy channels were: 10 - 25 keV, 25 - 50 keV, 50 - 100 keV, 100 - 300 keV, 300 keV - 1 MeV and 10 keV - 1 MeV. The BGO energy channels were 100 - 300 keV, 300 keV - 1 MeV, 1 - 40 MeV, and 200 keV - 40 MeV.

## 3. Temporal and spectral analysis

### 3.1 Pulse fitting

Temporal analysis was achieved within the ten energy channels by fitting the pulses with the Norris function [4], shown in Equation 1 and the goodness of the fits was measured with the reduced  $\chi^2$ . The rising and decaying times of the pulses are given by  $t_{rise}$  and  $t_{fall}$  respectively, and are connected by the peak time,  $t_{peak}$ . Additionally,  $A$  is the rate given in counts per second, and the exponents  $\nu_1$  and  $\nu_2$  are constants. The rise times of the SGRTs are presented in the results and discussion section.

$$I(t) = \begin{cases} A \exp \left[ - \left( \frac{|t-t_{peak}|}{t_{rise}} \right)^{\nu_1} \right]; & t < t_{peak} \\ A \exp \left[ - \left( \frac{|t-t_{peak}|}{t_{fall}} \right)^{\nu_2} \right]; & t > t_{peak} \end{cases} \quad (1)$$

### 3.2 Time-integrated and time-resolved spectral analysis

Time-integrated analysis was performed on all sources within the time interval when the main emission was observed. We also conducted time-resolved analysis by slicing the time intervals of multi-peaked SGRBs and sources that show pulse variability into smaller intervals. Both types of analyses were performed within the two energy ranges: 10 keV - 1 MeV and 200 keV - 40 MeV. The spectra of the SGRTs were retrieved from the *RMFIT* software<sup>3</sup> and were fit with the Comp model which breaks at  $E_{peak}$  and has a PL index of  $\alpha$ .

$$f_{Comp}(E) = \left( \frac{E}{100} \right)^\alpha \exp \left( - \frac{E(\alpha + 2)}{E_{peak}} \right) \quad (2)$$

## 4. Results and discussion

As stated in the introduction, the goal of this study is to be able to identify MGFs from an SGRB sample, which was accomplished by temporally and spectrally analysing the SGRTs. Each peak of GRB090510 and GRB210323A was fit within the same time interval as used in the spectral analysis. For instance, GRB090510 peak 1 in Figure 1 occurs at 0.508 - 0.626 s in Table 1. We fit 21 pulses with the Norris function, however, there were missing data points in some of the energy

<sup>2</sup><https://fermi.gsfc.nasa.gov/ssc/data/access/>

<sup>3</sup>[https://fermi.gsfc.nasa.gov/ssc/data/analysis/rmfit/vc\\_rmfit\\_tutorial.pdf](https://fermi.gsfc.nasa.gov/ssc/data/analysis/rmfit/vc_rmfit_tutorial.pdf)

channels corresponding to peaks that are not prominent enough for pulse fitting in those energy channels.

The  $t_{rise}$  values (see Figure 1) depict that the SGRBs have slower rise times, lasting a few hundreds of milliseconds. This implies that their flux takes a few hundreds of milliseconds to rise from  $\sim 10^{12}$  cm from their central engines. However, the brightest source in the sample, GRB090510, deviates from this pattern and has rapid  $t_{rise}$  values. This could be due to its peculiar Lorentz factor of  $\approx 1000$  [7], which decreases its radial timescale substantially. The MGF, on the other hand, has rapid rise times, which are a few tens of milliseconds as found by Burns et al. [3].

Both GRB090510 and GRB20041515A display similar  $t_{rise}$  values, suggesting that both of their emissions experienced an unexpected shift, resulting in rapid flux changes. Moreover, the processes responsible for both sources might be the same, further implying that MGFs could be one of the central engines of SGRBs, as proposed by Nakar [8].

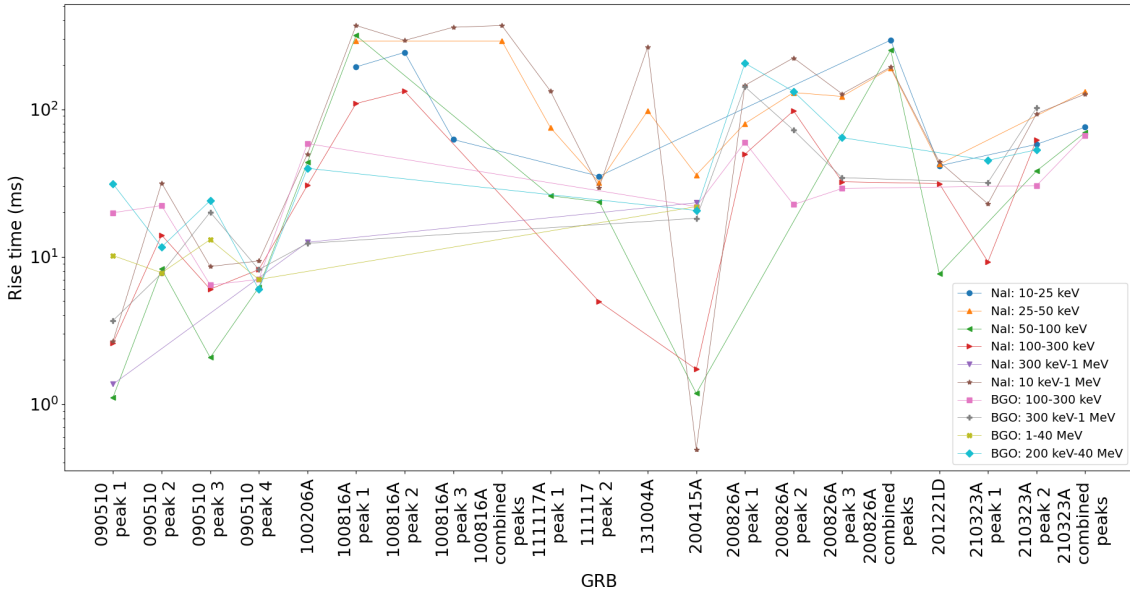


**Figure 1:** Pulse rise time plot of SGRBs and the MGF, GRB200415A, in ten energy channels within the range 10 keV – 40 MeV. The lines connect sources within the same energy channel.

The spectra of the SGRTs were best fit with the Comp model, and we tabulated its parameters in Table 1. All the transients are spectrally hard, although the MGF has the hardest spectrum with a PL index,  $\alpha = -0.01 \pm 0.11$ , associated with a C-stat/dof value of 299/237 in agreement with other studies (see [10] and [11]). The Comp model is a non-thermal spectral model, hence the SGRTs have a non-thermal spectrum. The MGF, however, it has the hardest spectrum, indicating that its spectrum is neither non-thermal nor purely thermal, but more thermal-like. GRB200415A’s hard spectrum is due to thermal-like emissions, which are quickly dissipated from its magnetar surface in a narrow region. The non-thermal spectra of the SGRBs are due to non-thermal radiating electrons from synchrotron emission.

The PL index distribution of the SGRBs is within  $-1.48 < \alpha < -0.37$ , and 50% of them violate the synchrotron limits [9] as shown in the *left* panel of Figure 2. This suggests that there are other mechanisms might account for the hard  $\alpha$  that lies outside the synchrotron limits. The *right* panel

of Figure 2 indicates the time-integrated spectra of the SGRBs modelled with the Comp model. The figure also displays that their spectra peaks at a few MeV and are comparable for both the SGRBs and the MGF. Therefore, the radiating electrons from both transients are accelerated to comparable energies. This requires Lorentz factors with 100 and 1000 [8]. Moreover, SGRBs have high intrinsic isotropic energies of  $E_{iso} \approx 10^{52}$  erg, while the MGF is less energetic with  $E_{iso} \approx 10^{44}$  erg.

GRB	Time interval (s)	Detector(s)	$\alpha$	$E_{peak}$ (keV)	$E_{iso}$ (erg)	C-stat/dof
090510	0.508 – 0.626	n6 + b1	$-0.63 \pm 0.05$	$2732 \pm 246$	$(1.31 \pm 0.07) \times 10^{53}$	181/236
	0.624 – 0.70		$-0.37 \pm 0.08$	$5202 \pm 422$	$(1.82 \pm 0.11) \times 10^{53}$	262/236
	0.702 – 0.786		$-1.07 \pm 0.06$	$12270 \pm 3380$	$(5.31 \pm 0.50) \times 10^{52}$	256/236
	0.798 – 0.90		$-1.17 \pm 0.09$	$2571 \pm 1240$	$(2.14 \pm 0.46) \times 10^{51}$	213/236
	0.508 – 0.90		$-0.81 \pm 0.03$	$4786 \pm 323$	$(9.09 \pm 0.30) \times 10^{52}$	198/236
100206A	-0.176 – 0.224	n5 + b0	$-0.61 \pm 0.22$	$651.5 \pm 180.0$	$(2.12 \pm 0.41) \times 10^{50}$	303/236
100816A	-1.488 – 3.448	n7	$-0.40 \pm 0.15$	$140.6 \pm 12.3$	$(2.35 \pm 0.16) \times 10^{51}$	111/112
111117A	-0.160 – 0.544	n6	$-0.58 \pm 0.38$	$533.50 \pm 367.00$	$(3.12 \pm 0.71) \times 10^{50}$	131/112
131004A	-0.400 – 0.992	na	$-1.48 \pm 0.26$	$102.80 \pm 44.80$	$(3.12 \pm 0.71) \times 10^{50}$	124/110
<b>200415A</b>	<b>-0.128 – 0.384</b>	<b>n3 + b0</b>	<b><math>-0.01 \pm 0.11</math></b>	<b><math>1017 \pm 70</math></b>	<b><math>(5.28 \pm 1.97) \times 10^{44}</math></b>	<b>299/237</b>
200826A	0.00 – 0.992	n7 + b1	$-0.86 \pm 0.06$	$140.40 \pm 5.71$	$(7.45 \pm 0.19) \times 10^{51}$	317/233
201221D	-0.112 – 0.208	n7	$-0.54 \pm 0.27$	$127.20 \pm 20.10$	$(6.88 \pm 1.20) \times 10^{50}$	97/111
210323A	-0.112 – 0.032	n5 + b0	$-0.50 \pm 0.26$	$2085 \pm 616$	$(3.15 \pm 0.82) \times 10^{51}$	233/236
	0.016 – 0.240		$-1.17 \pm 0.07$	$1859 \pm 606$	$(3.88 \pm 0.63) \times 10^{51}$	222/236
	-0.112 – 0.240		$-1.05 \pm 0.07$	$2066 \pm 518$	$(3.61 \pm 0.50) \times 10^{51}$	237/236

**Table 1:** Time-resolved and time-integrated spectral fit results for all the sources including the MGF (in bold) using the Comp model.

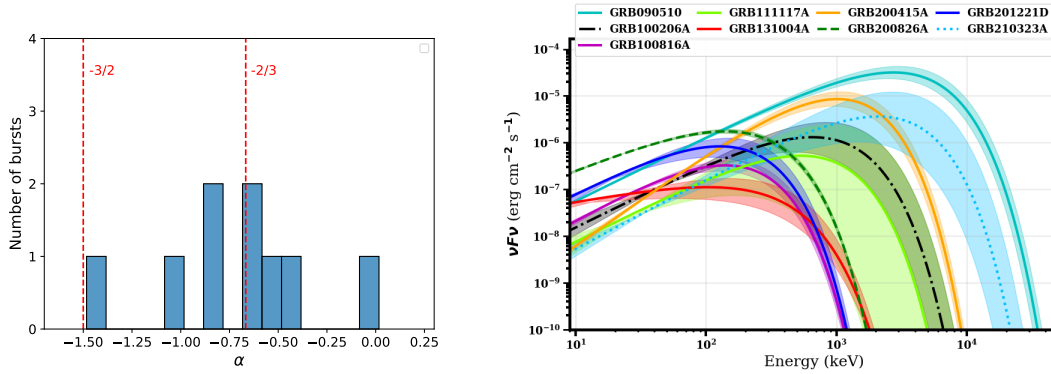


**Figure 2:** Time-integrated PL index distribution (left panel) and time-integrated spectra (right panel). The  $\alpha = -\frac{3}{2}$  vertical line is the synchrotron adiabatic cooling limit, and  $\alpha = -\frac{2}{3}$  is the synchrotron "line of death".

## 5. Conclusion

In this study, we have shown that the MGF, GRB200415A, has rapid  $t_{rise}$  values and a harder spectrum, while the SGRBs have slower  $t_{rise}$  values with soft spectra. From these observations, we conclude that the thermal-like emissions of MGFs have rapidly rising fluxes with  $t_{rise}$  values within a few tens of milliseconds. While we focused on one MGF, only a few are misclassified as

SGRBs. Burns et al. [3] also confirmed that their  $t_{rise}$  values are within a few tens of milliseconds. Additionally, SGRBs have slower rise times, implying that their non-thermal emissions requires hundreds of milliseconds to experience a flux increase. This study can also be used to identify MGFs from an SGRB sample based on their pulse rise time and their PL spectral index, without knowing their redshift.

## Acknowledgments

We acknowledge support from the National Research Foundation for funding this research and the *Fermi* Science Support Center for developing tools that were essential to carry out this study.

## References

- [1] T. Piran, The physics of gamma-ray bursts, *Reviews of Modern Physics* 76 (4) (2005) 1143.
- [2] R.W. Klebesadel, I.B. Strong, and R.A. Olson, Observations of gamma-ray bursts of cosmic origin, *The Astrophysical Journal* 182 (1973) L85
- [3] E. Burns, D. Svinkin, K. Hurley, Z. Wadiasingh, M. Negro, G. Younes, R. Hamburg, A. Ridnaia, D. Cook, S. Cenko, et al., Identification of a local sample of gamma-ray bursts consistent with a magnetar giant flare origin, *The Astrophysical Journal Letters* 907 (2) (2021) L28
- [4] J. P. Norris, R. J. Nemiroff, J. T. Bonnell et al., Attributes of pulses in long bright gamma-ray bursts, *The Astrophysical Journal* 459 (1996) 393.
- [5] T. Piran, Gamma-ray bursts and the fireball model, *Physics Reports* 314 (6) (1999) 575–667
- [6] C. Meegan, G. Lichti, P. N. Bhat et al., The Fermi gamma-ray burst monitor, *The Astrophysical Journal* 702 (1) (2009) 791.
- [7] M. Ackermann, K. Asano, W. B. Atwood et al., Fermi observations of grb 090510: A short-hard gamma-ray burst with an additional, hard power-law component from 10 keV to GeV energies, *The Astrophysical Journal* 716 (2) (2010) 1178.
- [8] E. Nakar, Short-hard gamma-ray bursts, *Physics Reports* 442 (1-6) (2007) 166–236.
- [9] J. I. Katz, Low frequency spectra of gamma-ray bursts, *The Astrophysical Journal* 432 (1993) L107.
- [10] O. J. Roberts, P. Veres, M. G. Baring, M. S. Briggs, C. Kouveliotou, E. Bissaldi, G. Younes, S. I. Chastain, S. J. DeLaunay, D. Huppenkothen, et al., Rapid spectral variability of a giant flare from a magnetar in NGC 253, *Nature* 589 (7841) (2021) 207–210.
- [11] D. Svinkin, D. Frederiks, K. Hurley, R. Aptekar, S. Golenetskii, A. Lysenko, A. V. Ridnaia, A. Tsvetkova, M. Ulanov, T. L. Cline, et al., A bright  $\gamma$ -ray flare interpreted as a giant magnetar flare in NGC 253, *Nature* 589 (7841) (2021) 211–213.